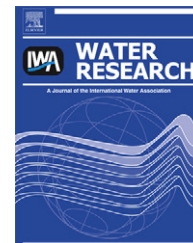


Available at www.sciencedirect.comjournal homepage: www.elsevier.com/locate/watres

Degradation of the antibiotic amoxicillin by photo-Fenton process – Chemical and toxicological assessment

Alam G. Trouó^{a,1}, Raquel F. Pupo Nogueira^{a,*}, Ana Agüera^b, Amadeo R. Fernandez-Alba^b, Sixto Malato^c

^a UNESP – Univ Estadual Paulista, Instituto de Química de Araraquara, CP 355, 14801-970, Araraquara, SP, Brazil

^b Pesticide Residues Group, University of Almería, 04120 Almería, Spain

^c Plataforma Solar de Almería, CIEMAT, P.O. Box 22, 04200 Tabernas, Almería, Spain

ARTICLE INFO

Article history:

Received 10 May 2010

Received in revised form

12 August 2010

Accepted 25 October 2010

Available online 31 October 2010

Keywords:

Pharmaceuticals

Wastewater

Advanced oxidation processes

Hydrolysis

LC-TOF-MS

Degradation pathway

ABSTRACT

The influence of iron species on amoxicillin (AMX) degradation, intermediate products generated and toxicity during the photo-Fenton process using a solar simulator were evaluated in this work. The AMX degradation was favored in the presence of the potassium ferrioxalate complex (FeOx) when compared to FeSO₄. Total oxidation of AMX in the presence of FeOx was obtained after 5 min, while 15 min were necessary using FeSO₄. The results obtained with *Daphnia magna* bioassays showed that the toxicity decreased from 65 to 5% after 90 min of irradiation in the presence of FeSO₄. However, it increased again to a maximum of 100% after 150 min, what indicates the generation of more toxic intermediates than AMX, reaching 45% after 240 min. However, using FeOx, the inhibition of mobility varied between 100 and 70% during treatment, probably due to the presence of oxalate, which is toxic to the neonates. After 240 min, between 73 and 81% TOC removal was observed. Different pathways of AMX degradation were suggested including the opening of the four-membered β-lactamic ring and further oxidations of the methyl group to aldehyde and/or hydroxylation of the benzoic ring, generating other intermediates after bond cleavage between different atoms and further oxidation to carboxylates such acetate, oxalate and propionate, besides the generation of nitrate and ammonium.

© 2010 Elsevier Ltd. All rights reserved.

1. Introduction

The presence of pharmaceuticals in the environment has been reported as an emerging risk to the biotic environment. Among the pharmaceuticals, special attention is focused on antibiotics, since bacterial resistance and toxic effects on several organisms such as algae and crustaceans have been found not only at high concentrations, but also at low concentrations resulting in chronic effects (Andreozzi et al.,

2004; Foti et al., 2009). The antibiotic AMX, a broad spectrum aminopenicillin antibiotic, widely used in human and veterinary medicine, was tested for toxicity on microalgal species (growth inhibition) and found to be nontoxic to *Pseudokirkneriella subcapitata* e *Closterium ehrenbergii* (EC₅₀ 100 mg L⁻¹), but showed marked toxicity to the *Synechococcus leopolensis* (EC₅₀ 2 μg L⁻¹) (Andreozzi et al., 2004). This compound has been identified in municipal sewage treatment plant effluent at concentration of 13 ng L⁻¹ in Italy (Castiglioni et al., 2006). So,

* Corresponding author. Tel.: +55 16 3301 9606; fax: +55 16 3301 6692.

E-mail address: nogueira@iq.unesp.br (R.F. Pupo Nogueira).

¹ Present address: UFU – Universidade Federal de Uberlândia, Instituto de Química, Av. João Naves de Ávila, 2121, CP 593, 38400-902, Uberlândia, MG, Brazil.

0043-1354/\$ – see front matter © 2010 Elsevier Ltd. All rights reserved.

doi:10.1016/j.watres.2010.10.029

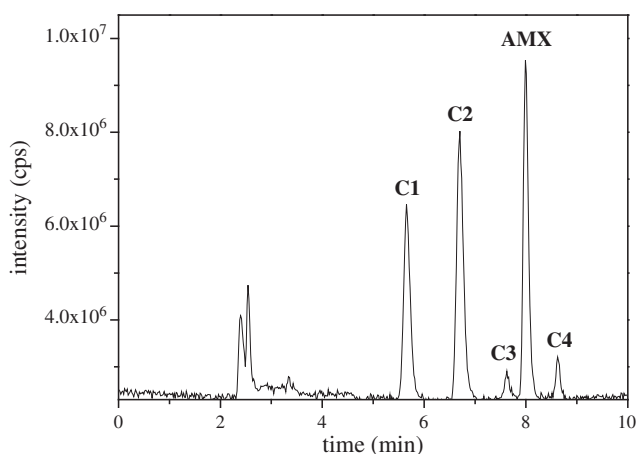


Fig. 1 – LC/TOF-MS chromatogram obtained from hydrolysis of AMX solution (10 mg L^{-1}) in water after 90 min at pH 2.5 in the dark.

it is necessary to evaluate new alternatives to prevent water contamination, considering the risks that residual pharmaceuticals can present to human health and to the environment.

The use of solar advanced oxidation processes (AOPs), such as photo-Fenton for the treatment of non-biodegradable and/or toxic compounds can be an alternative to the conventional processes. Previous works has shown the efficiency of this process on the degradation of different therapeutic classes of pharmaceuticals such as antibiotics, anti-inflammatory and analgesic drugs (Pérez-Estrada et al., 2005, 2007; Shemer et al., 2006; Bautitz and Nogueira, 2007; Trovó et al., 2008, 2009).

Some authors have reported fast and effective degradation of AMX under different conditions, such O_3 , $\text{O}_3/\text{H}_2\text{O}_2$, $\text{H}_2\text{O}_2/\text{UV}$, TiO_2 , Fenton and photo-Fenton (Arslan-Alaton and Dogruel, 2004; Arslan-Alaton and Caglayan, 2005; Andreozzi et al., 2005; Elmolla and Chaudhuri, 2009; Mavronikola et al., 2009; Martins et al., 2009). Arslan-Alaton and Dogruel (2004) applied a variety of advanced oxidation processes, $\text{O}_3/\text{OH}^\cdot$, $\text{H}_2\text{O}_2/\text{UV}$, $\text{Fe}^{2+}/\text{H}_2\text{O}_2$, $\text{Fe}^{3+}/\text{H}_2\text{O}_2$, $\text{Fe}^{2+}/\text{H}_2\text{O}_2/\text{UV}$, $\text{Fe}^{3+}/\text{H}_2\text{O}_2/\text{UV}$, to penicillin formulation effluent, concluding that best results regarding complete removal of active substance AMX were obtained using the photo-Fenton process and alkaline ozonation. Although the literature reports the efficiency of AMX degradation by different treatments, no studies have been published on its treatment by solar photo-Fenton, including intermediates generated and evolution of toxicity.

The aim of the present work was to study the use of the photo-Fenton process for the degradation of AMX using a solar simulator. The study includes the influence of the iron species used, the identification of the intermediate products generated during the process by the use of liquid chromatography coupled to time-of-flight mass spectrometry (LC-TOF-MS) and the toxicity assessment.

2. Experimental

2.1. Chemicals

All the AMX solutions were prepared in distilled water. AMX was purchased from Sigma–Aldrich and used as received. Hydrogen peroxide (30% w/v) (POCH, SA), $\text{FeSO}_4 \cdot 7\text{H}_2\text{O}$ and sulphuric acid (POCH, SA), NaOH and bovine liver catalase (Sigma–Aldrich) were also used as received. Potassium ferrioxalate ($\text{K}_3\text{Fe}(\text{C}_2\text{O}_4)_3 \cdot 3\text{H}_2\text{O}$), named as FeOx, was prepared and purified as described previously (Hatchard and Parker, 1956) using iron nitrate and potassium oxalate (Mallinckrodt). Ammonium metavanadate (Sigma–Aldrich) solution was prepared at a concentration of 0.060 M in 0.36 M H_2SO_4 . All reagents were of analytical grade. HPLC-grade acetonitrile and methanol (Merck) and formic acid (Fluka) were used for HPLC analyses.

2.2. Hydrolysis, photolysis and photo-Fenton experiments

The solutions for hydrolysis and photolysis experiments were prepared by dissolving AMX in distilled water at an initial concentration of 10 mg L^{-1} (TOC 5.3 mg C L^{-1} , natural pH 6.2). Hydrolysis experiments were performed in 250 mL beakers at two different pH (2.5 and 6.2). The beakers were kept in the dark at room temperature for 330 min. The photolysis and photo-Fenton experiments were conducted in a solar simulator (Suntest CPS+ from Heraeus, Germany) equipped with a 1100 W xenon arc lamp and special filters restricting transmission of light below 290 nm. The lamp was set to minimum intensity (250 W m^{-2}), since under high intensity the intermediates generated could be quickly degraded making difficult their detection. Pyrex glass vessels (Schott Durand, Germany) provided with an internal recirculating water system were used to maintain the internal temperature at $25 \pm 2 \text{ }^\circ\text{C}$.

The initial AMX concentration for the photo-Fenton experiments was 50 mg L^{-1} (TOC = 26.3 mg C L^{-1}). Although this concentration is higher than that found in aqueous

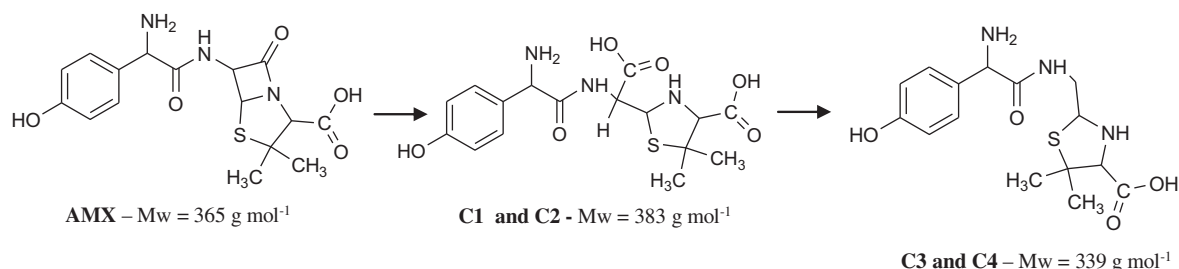


Fig. 2 – Products of AMX hydrolysis in water.

Table 1 – Accurate mass measurements found by LC-ESI-TOF-MS spectra of protonated AMX degradation products and fragmentation ions by hydrolysis in water.

Compound	Retention time (min)	Formula	Calculated mass (<i>m/z</i>)	Expected Mass (<i>m/z</i>)	Error (ppm)	*DBE		
C1	5.563	C ₁₆ H ₂₂ N ₃ O ₆ S	384.1222	384.1223	−0.48	7.5		
		C ₁₆ H ₂₁ N ₃ O ₆ NaS	406.1007	406.1043	−8.9	7.5		
		C ₁₆ H ₁₉ N ₂ O ₆ S	367.0952	367.0958	−1.7	8.5		
		C ₁₅ H ₂₂ N ₃ O ₄ S	340.1317	340.1325	2.5	6.5		
		C ₁₅ H ₁₉ N ₂ O ₄ S	323.1057	323.106	−0.94	7.5		
		C ₇ H ₁₃ N ₂ O ₂ S	189.0687	189.0692	−2.8	2.5		
		C ₆ H ₁₀ NO ₂ S	160.0420	160.0426	−4.2	2.5		
		C2	6.613	C ₁₆ H ₂₂ N ₃ O ₆ S	384.1229	384.1223	1.3	7.5
				C ₁₆ H ₁₉ N ₂ O ₆ S	367.0964	367.0958	1.5	8.5
C ₁₅ H ₂₂ N ₃ O ₄ S	340.1323			340.1325	−0.75	6.5		
C ₁₅ H ₁₉ N ₂ O ₄ S	323.1063			323.106	0.91	7.5		
C ₇ H ₁₃ N ₂ O ₂ S	189.0694			189.0692	0.92	2.5		
C ₆ H ₁₀ NO ₂ S	160.0435			160.0426	5.1	2.5		
C3	7.572			C ₁₅ H ₂₂ N ₃ O ₄ S	340.1325	340.1325	−0.16	6.5
				C ₁₅ H ₂₁ N ₃ O ₄ NaS	362.1158	362.1444	3.6	6.5
				C ₁₅ H ₁₉ N ₂ O ₄ S	323.1057	323.106	−0.94	7.5
		C ₁₄ H ₁₉ N ₂ O ₃ S	295.1105	295.111	−2.0	6.5		
		C ₉ H ₁₃ N ₂ O ₃ S	229.0642	229.0641	0.26	4.5		
		C ₇ H ₁₃ N ₂ O ₂ S	189.0687	189.0692	−2.8	2.5		
		C ₉ H ₁₁ N ₂ O	163.0861	163.0865	−3.0	5.5		
		C ₇ H ₇ O	107.0491	107.0491	−0.39	4.5		
		AMX	7.897	C ₁₆ H ₂₀ N ₃ O ₅ S	366.1114	366.1118	−1.1	8.5
C ₁₆ H ₁₉ N ₃ O ₅ NaS	388.0919			388.0937	−4.8	8.5		
C ₁₆ H ₁₇ N ₂ O ₅ S	349.0849			349.0852	−1.1	9.5		
C ₁₅ H ₁₇ N ₂ O ₄ S	321.0894			321.0903	3.0	8.5		
C ₁₀ H ₁₀ NO ₂ S	208.0420			208.0426	−3.2	6.5		
C ₆ H ₁₀ NO ₂ S	160.0433			160.0426	3.9	2.5		
C ₄ H ₄ NOS	114.0006			114.0008	1.8	3.5		
C4	8.675			C ₁₅ H ₂₂ N ₃ O ₄ S	340.1331	340.1325	1.6	6.5
				C ₁₅ H ₂₁ N ₃ O ₄ NaS	362.1149	362.1144	1.1	6.5
		C ₁₅ H ₁₉ N ₂ O ₄ S	323.1065	323.106	1.5	7.5		
		C ₁₄ H ₁₉ N ₂ O ₃ S	295.1112	295.111	0.37	6.5		
		C ₉ H ₁₃ N ₂ O ₃ S	229.0623	229.0641	−8.0	4.5		
		C ₇ H ₁₃ N ₂ O ₂ S	189.0700	189.0692	4.1	2.5		
		C ₉ H ₁₁ N ₂ O	163.0869	163.0865	1.9	5.5		
		C ₇ H ₇ O	107.0502	107.0491	9.9	4.5		

* DBE = double-bond equivalency.

environment, it was chosen to permit an adequate detection of intermediates. The initial concentration of FeSO₄·7H₂O or FeOx was 0.05 mM, which is below the maximum concentration of iron allowed in wastewater according to Brazilian legislation. Based on previous work (Trovó et al., 2009), the initial H₂O₂ concentration used was 120 mg L^{−1} and new additions of H₂O₂ were made during the experiments according to the consumption of H₂O₂. The initial pH was adjusted to between 2.5–2.8, the optimum pH range for the photo-Fenton process.

2.3. Chemical analysis

Before LC-MS analysis, the solution pH was adjusted to between 6 and 8, and 0.5 mL catalase solution (0.1 g L^{−1}) was added to 25 mL of sample to quench the reaction and guarantee the absence of hydrogen peroxide before the bioassays. The samples were then filtered through 0.45 μm membranes. The AMX concentrations and intermediates were analysed by liquid chromatography electrospray time-of-flight mass

spectrometry (LC-ESI-TOF-MS), in positive ionisation mode, using an HPLC (Agilent Series 1100) equipped with a 3 × 250 mm reverse-phase C₁₈ analytical column, 5 μm particle size (Zorbax SB-C₁₈, Agilent Technologies). A and B mobile phases were acetonitrile and water with 0.1% formic acid, respectively, at a flow rate of 0.4 mL min^{−1}. The injection volume was 20 μL. A linear gradient progressed from 10% A (initial conditions) to 100% A in 50 min, and was maintained at 100% A for 3 min. A 15 min post-run time back to the initial mobile-phase composition was allowed after each analysis. Under these conditions, AMX retention time was between 7.9 and 8.2 min, with a detection limit of 5 μg L^{−1}. This HPLC system was connected to an Agilent MSD time-of-flight mass spectrometer with an electrospray interface operating under the following conditions: capillary, 4000 V; nebulizer, 40 psi; drying gas, 7.0 L min^{−1}; gas temperature, 300 °C; skimmer voltage, 60 V; octapole dc1, 36.5 V; octapole rf, 250 V; fragmentor, 190 V.

The mineralization of AMX during the experiments was evaluated by measuring the decay of the total organic carbon (TOC) using a TOC analyser (Shimadzu TOC 5050A) equipped with

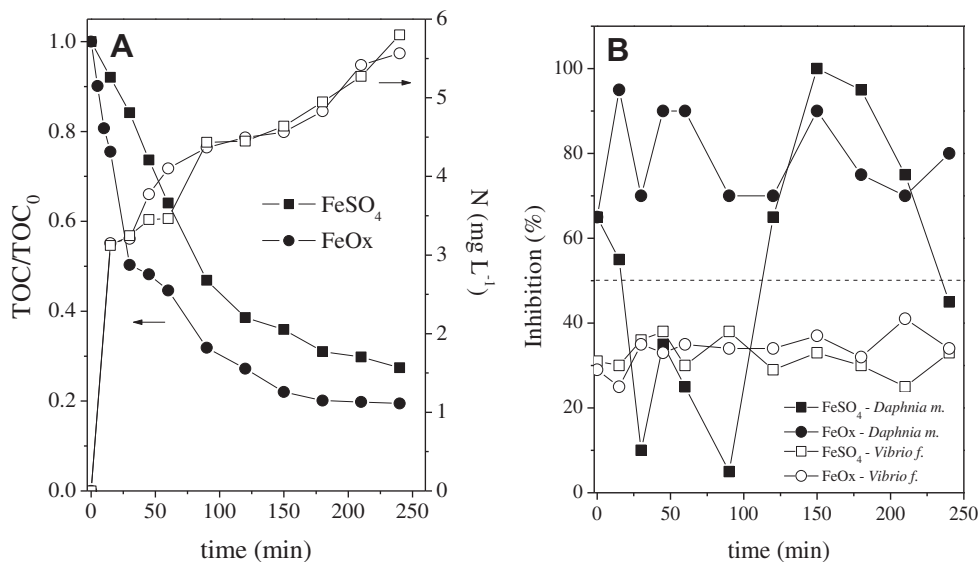


Fig. 3 – Influence of iron species on the (A) removal of TOC (solid symbols) and release of nitrogen (open symbols), (B) evolution of toxicity during AMX photo-Fenton treatment using *Daphnia magna* (48 h) and *Vibrio fischeri* (30 min) bioassays. Initial concentrations: [AMX] = 50 mg L⁻¹ (26.3 mg L⁻¹ TOC); [Fe²⁺] = 0.05 mM; [H₂O₂] = 120 mg L⁻¹ (further additions); pH = 2.5.

an ASI5000 autosampler. Ammonium, carboxylates and NO₃ concentrations were measured with a Dionex DX-600 ion chromatograph using a Dionex Ionpac AS 11-HC 4 mm × 250 mm column. The gradient program was pre-run for 5 min with 20 mM

NaOH, 8 min with 20 mM NaOH and 7 min with 35 mM NaOH, at a flow rate of 1.5 mL min⁻¹.

The hydrogen peroxide was measured during the experiments using the spectrophotometric method employing

Table 2 – Accurate mass measurements found by LC-ESI-TOF-MS spectra of protonated AMX degradation products and fragmentation ions by photo-Fenton process in water with solar simulator.

Compound	Retention time (min)	Formula	Calculated mass (m/z)	Expected mass (m/z)	Error (ppm)	*DBE
C5	4.187	C ₁₆ H ₂₀ N ₃ O ₆ S	382.1069	382.1067	0.43	8.5
		C ₁₆ H ₁₇ N ₂ O ₆ S	365.0808	365.0801	1.7	9.5
		C ₁₅ H ₁₇ N ₂ O ₅ S	337.0857	337.0852	1.3	8.5
		C ₁₂ H ₁₁ N ₂ O ₄	247.0715	247.0713	0.67	8.5
		C ₆ H ₁₀ NO ₂ S	160.0432	160.0432	-0.16	2.5
C6	4.513	C ₁₆ H ₂₂ N ₃ O ₇ S	400.1170	400.1172	-0.75	7.5
		C ₁₆ H ₁₉ N ₂ O ₇ S	383.0916	383.0907	2.2	8.5
		C ₁₆ H ₁₇ N ₂ O ₆ S	365.0792	365.0801	-2.7	9.5
		C ₁₅ H ₁₉ N ₂ O ₅ S	339.1013	339.1009	1.1	7.5
		C ₈ H ₁₅ N ₂ O ₄ S	235.0754	235.0747	2.9	2.5
		C ₆ H ₁₀ NO ₂ S	160.0431	160.0426	2.6	2.5
		C ₇ H ₈ NO	122.0598	122.0600	-2.0	4.5
C1	5.549	C ₁₆ H ₂₂ N ₃ O ₆ S	384.1222	384.1223	-0.48	7.5
		C ₁₆ H ₂₁ N ₃ O ₆ NaS	406.1041	406.1043	-0.56	7.5
		C ₁₆ H ₁₉ N ₂ O ₆ S	367.0955	367.0958	-0.91	8.5
		C ₁₅ H ₂₂ N ₃ O ₄ S	340.1309	340.1325	-4.9	6.5
		C ₁₅ H ₁₉ N ₂ O ₄ S	323.1069	323.1060	2.8	7.5
		C ₇ H ₁₃ N ₂ O ₂ S	189.0694	189.0692	0.92	2.5
		C ₆ H ₁₀ NO ₂ S	160.0430	160.0426	2.0	2.5
C7	5.906	C ₁₆ H ₂₀ N ₃ O ₆ S	382.1066	382.1067	-0.35	8.5
		C ₁₆ H ₁₇ N ₂ O ₆ S	365.0794	365.0801	-2.1	9.5
		C ₁₀ H ₁₀ NO ₃ S	224.0370	224.0375	-2.6	6.5
		C ₇ H ₁₃ N ₂ O ₂ S	189.0686	189.0692	-3.3	2.5
		C ₆ H ₁₀ NO ₂ S	160.0422	160.0426	-3.0	2.5
		C ₄ H ₄ NOS	114.0011	114.0008	2.5	3.5

(continued on next page)

Table 2 (continued).

Compound	Retention time (min)	Formula	Calculated mass (m/z)	Expected mass (m/z)	Error (ppm)	*DBE
C2	7.010	C ₁₆ H ₂₂ N ₃ O ₆ S	384.1223	384.1223	−0.22	7.5
		C ₁₆ H ₁₉ N ₂ O ₆ S	367.0958	367.0958	−0.095	8.5
		C ₁₅ H ₂₂ N ₃ O ₄ S	340.1317	340.1325	−2.5	6.5
		C ₁₅ H ₁₉ N ₂ O ₄ S	323.1063	323.1060	0.91	7.5
		C ₇ H ₁₃ N ₂ O ₂ S	189.0682	189.0692	−5.4	2.5
		C ₆ H ₁₀ NO ₂ S	160.0425	160.0426	−1.1	2.5
		C ₅ H ₈ NS	114.0369	114.0371	−2.6	2.5
		C ₄ H ₁₀ NO	88.0755	88.0756	−22	0.5
		C3	7.969	C ₁₅ H ₂₂ N ₃ O ₄ S	340.1321	340.1325
C ₁₅ H ₁₉ N ₂ O ₄ S	323.1049			323.1060	−3.4	7.5
C ₇ H ₁₃ N ₂ O ₂ S	189.0693			189.0692	0.39	2.5
C ₉ H ₁₁ N ₂ O	163.0866			163.0865	0.064	5.5
C4	8.909	C ₁₅ H ₂₂ N ₃ O ₄ S	340.1324	340.1325	−0.45	6.5
		C ₁₅ H ₁₉ N ₂ O ₄ S	323.1063	323.1060	0.91	7.5
		C ₁₄ H ₁₉ N ₂ O ₃ S	295.1100	295.1110	−3.7	6.5
		C ₁₀ H ₉ N ₂ O ₂ S	189.0667	189.0658	4.5	7.5
		C ₉ H ₁₁ N ₂ OS	163.0880	163.0865	8.6	5.5
C8	9.941	C ₁₅ H ₂₀ N ₃ O ₅ S	354.1132	354.1118	3.9	7.5
		C ₁₅ H ₁₇ N ₂ O ₅ S	337.0855	337.0852	0.68	8.5
		C ₁₅ H ₁₅ N ₂ O ₄ S	319.0744	319.0747	−0.96	9.5
		C ₁₄ H ₁₇ N ₂ O ₃ S	293.0957	293.0954	0.88	7.5
		C ₉ H ₉ N ₂ O ₃	193.0611	193.0607	1.7	6.5
		C ₆ H ₁₁ N ₂ OS	159.0586	159.0586	−0.38	2.5
		C ₅ H ₈ NOS	130.0322	130.0321	0.68	2.5
		C ₇ H ₇ O	107.0493	107.0491	1.5	4.5
C9	10.2	C ₁₄ H ₂₀ N ₃ O ₃ S	310.1225	310.1219	1.6	6.5
		C ₁₄ H ₁₇ N ₂ O ₃ S	293.0953	293.0954	−0.48	7.5
C10	10.701	C ₈ H ₁₁ N ₂ O ₄ NaS	231.0435	231.0434	0.41	4.5
		C ₈ H ₁₀ N ₂ O ₄ NaS	253.0262	253.0253	3.4	4.5
		C ₆ H ₁₀ NO ₂ S	160.0429	160.0426	1.4	2.5
C11	11.89	C ₅ H ₁₂ NO	102.0909	102.0913	−4.3	0.5
		C ₁₆ H ₁₈ N ₃ O ₉ S	428.0754	428.0758	−1.0	9.5
		C ₁₆ H ₁₇ N ₃ O ₉ NaS	450.0581	450.0577	0.73	9.5
		C ₁₆ H ₁₆ N ₃ O ₈ S	410.0660	410.0652	1.8	10.5
		C ₁₅ H ₁₈ N ₃ O ₇ S	384.0852	384.0859	−2.1	8.5
		C ₆ H ₁₀ NO ₂ S	160.0429	160.0426	1.4	2.5
C12	12.238	C ₄ H ₄ N ₃	94.0401	94.0399	1.3	4.5
		C ₁₄ H ₂₀ N ₃ O ₂ S	294.1273	294.127	0.76	6.5
		C ₁₄ H ₁₇ N ₂ O ₂ S	277.1008	277.1005	0.99	7.5
		C ₁₀ H ₉ N ₂ O ₂	189.0663	189.0658	2.4	7.5
		C ₁₀ H ₇ N ₂ O	171.0549	171.0552	−2.3	8.5
C13	12.71	C ₆ H ₁₀ NO ₃ S	176.0374	176.0375	−1.1	2.5
		C ₆ H ₈ NO ₂ S	158.0266	158.027	−2.7	3.5
		C ₅ H ₈ NOS	130.0320	130.0321	−0.86	2.5
		C ₄ H ₈ NS	102.0375	102.0371	3.0	1.5
C14	13.704	C ₁₆ H ₂₀ N ₃ O ₅ S	366.1116	366.1118	0.60	8.5
		C ₁₀ H ₁₁ N ₂ O ₃	207.0760	207.0764	−2.0	6.5
		C ₆ H ₁₀ NO ₂ S	160.0426	160.0426	−0.48	2.5
		C ₅ H ₈ NS	114.0369	114.0371	−2.6	2.5
C15	15.86	C ₁₆ H ₁₈ N ₃ O ₈ S	412.0811	412.0809	0.45	9.5
		C ₁₆ H ₁₇ N ₃ O ₈ NaS	434.0630	434.0628	3.3	9.5
		C ₁₀ H ₉ N ₂ O ₂	189.0670	189.0658	6.1	7.5
		C ₆ H ₁₀ NO ₂ S	160.0426	160.0426	−0.48	2.5
C16	16.382	C ₁₆ H ₁₉ N ₂ O ₇ S	383.0911	383.0907	0.91	8.5
		C ₁₆ H ₁₇ N ₂ O ₆ S	365.0795	365.0801	−1.9	9.5
		C ₁₅ H ₁₉ N ₂ O ₅ S	339.1011	339.1009	0.53	7.5
		C ₆ H ₁₀ NO ₂ S	160.0431	160.0426	2.6	2.5

* DBE = double-bond equivalency.

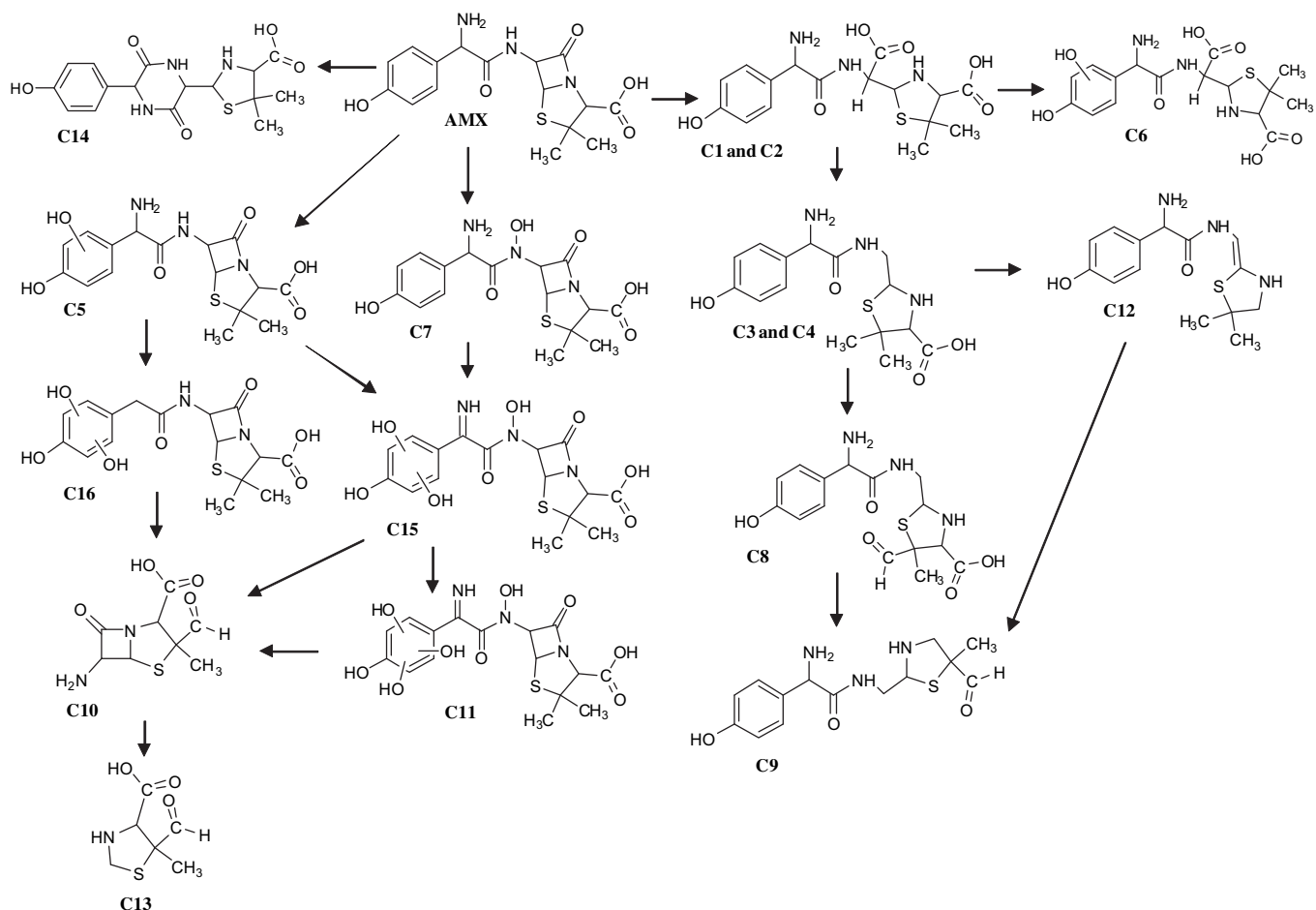


Fig. 4 – Proposed photo-Fenton degradation pathway of AMX in distilled water using different iron species.

ammonium metavanadate (Unicam-II spectrophotometer) as described by Nogueira et al. (2005a).

2.4. Toxicity evaluation

The same sample treatment described for the analysis by liquid chromatography was made prior to the toxicity evaluation. The toxicity tests were made with commercial bioassays, Biofix[®]Lumi-10, based on inhibition of the luminescence emitted by the marine bacteria *Vibrio fischeri*, and *Daphnia magna* immobilization (Daphtoxkit F[™] magna, Creasel, Belgium) as described previously by Trovó et al. (2009).

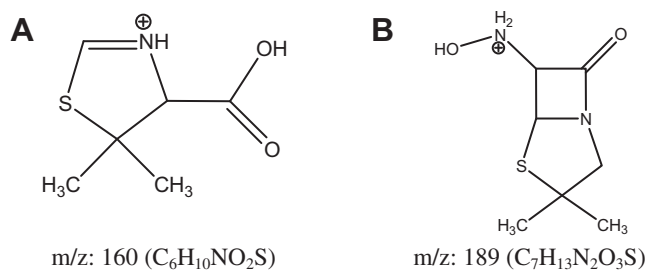


Fig. 5 – Proposed structures for fragments at m/z 160 and m/z 189.

3. Results and discussion

3.1. Hydrolysis and photolysis

Several blank experiments were performed at the initial AMX concentration of 10 mg L^{-1} , to assure that the results found during the photocatalytic tests were consistent and not due to hydrolysis and/or photolysis. No decay in AMX concentration during irradiation at natural pH (6.2) after 6 h irradiation was observed. However, 64% of AMX was hydrolyzed after 1.5 h reaching 74% after 5.5 h at pH 2.5 in the dark, while no hydrolysis at pH 6.2 was observed. However, no mineralization occurred after the same time, which indicates the generation of intermediates formed during hydrolysis at acid medium. Four intermediates were detected using LC/TOF-MS analysis (Fig. 1), not so interesting for the behavior of AMX in the environment but important for interpretation of photo-Fenton results.

The m/z of two intermediates detected was 340 and of other two 384. The hydrolysis of AMX starts with the opening of the four-membered β -lactam ring and yields the product AMX penicilloic acid with m/z 384 (C1 and C2), which contains a free carboxylic acid group. Then decarboxylation of the free carboxylic acid occurs, generating two intermediates with m/z

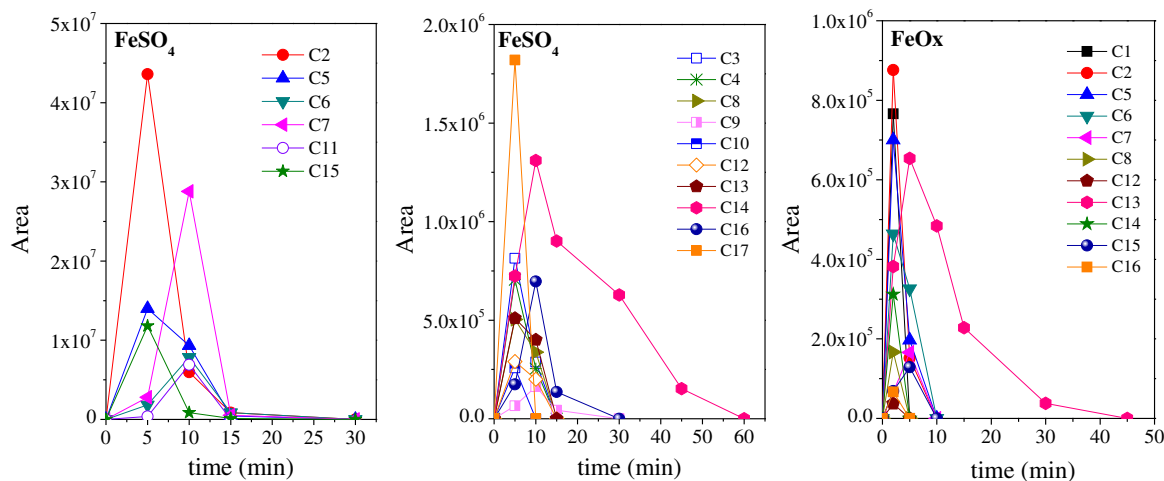


Fig. 6 – Evolution of the intermediates of AMX degradation in water by photo-Fenton process using different iron species.

340 (C3 and C4) (Fig. 2). These results are in accordance with the work of Nagele and Moritz (2005).

However, the products formed are stereoisomer compounds, what is demonstrated by the same fragmentation pattern of the ions for the two different retention times (Table 1). The literature reports a chromatographic method for the detection and determination of these stereoisomers (Valvo et al., 1998). The formation of these stereoisomers occurs with opening of the four-membered β -lactam ring, since the carbon between nitrogen and sulphur in the thiazolidine ring is chiral. In this way, during hydrolysis the formation of the respective stereoisomer occurs generating the products of m/z 340 [C3: amoxilloic acid (5S) and C4: amoxilloic acid (5R)] and the products of m/z 384 [C1: amoxicilloic acid (5S,6R) and C2: amoxicilloic acid (5R,6R)].

3.2. Photo-Fenton experiments

The efficiency of degradation to different classes of organic compounds can be influenced by the iron species (Nogueira et al., 2005b). Therefore, the influence of different iron species (FeOx and FeSO₄) on AMX degradation by photo-Fenton process was evaluated. A 50 mg L⁻¹ AMX solution in the presence of 0.05 mM of iron and 120 mg L⁻¹ H₂O₂ was irradiated. New additions of H₂O₂ were made when necessary.

The AMX oxidation and mineralization was favoured when FeOx was used as iron species. Total removal of AMX was observed after 5 min irradiation, while 15 min were necessary using FeSO₄ (data not shown). A similar behaviour was observed for the removal of TOC. However total mineralization was not observed. Under these conditions, a removal of 73 and 81% of TOC was achieved after 240 min in the presence of FeSO₄ and FeOx, respectively (Fig. 3A). The difference was more relevant at earlier stages, with a removal of 50% of TOC after 75 and 25 min in the presence of FeSO₄ and FeOx, respectively. Better results of AMX degradation were also observed when FeOx was used in comparison to Fe(NO₃)₃ (Trovó et al., 2008).

The nitrogen in the AMX molecule was released mainly as ammonium, expressed as total nitrogen in Fig. 3A. The total

nitrogen concentration released after 240 min corresponded to 100% of the theoretic amount, and this shows that the residual TOC after 240 min did not contain nitrogen (Fig. 3A). No difference on ammonium release rate was observed when different iron species were used. The main carboxylates identified during irradiation were: acetate, oxalate and propionate.

AMX (50 mg L⁻¹) caused 30% inhibition of *Vibrio fischeri* bioluminescence in bioassay after 30 min exposure. During the photo-Fenton degradation using the different iron species, no significant change in the toxicity was observed (Fig. 3B). However, using *Daphnia magna* bioassays, 65% inhibition of the neonates mobility (after 48 h of exposure) was observed in the initial AMX solution. After 90 min, the inhibition of mobility of the neonates decreased to 5% using FeSO₄. However, it increased again to a maximum of 100% after 150 min achieving 45% at the end of the experiment (240 min) (Fig. 3B). However, using FeOx, the inhibition of mobility varied between 95 and 70% during the treatment, probably due to the presence of oxalate, which is toxic to the neonates. A control experiment in the presence of only FeOx showed 100% of mobility inhibition. The increase of toxicity after 120 min was observed with both FeSO₄ and FeOx (Fig. 3B), what coincides with the plateau observed for TOC removal, suggesting that the toxicity is due to carboxylic acids generated during degradation process (Pintar et al., 2004).

3.3. Identification of intermediates and AMX degradation pathway in water by photo-Fenton process in a solar simulator

The identification of the main degradation products generated during the photo-Fenton treatment was carried out in order to propose a degradation pathway and assess the intermediates that possibly contribute to the toxicity. Analysis by LC-TOF-MS allowed the detection and identification of sixteen intermediates during AMX degradation by photo-Fenton process (Table 2). The main fragments observed in the mass spectra of each intermediate are indicated on Fig. 4. Among these intermediates, fifteen were detected when FeSO₄ was used

(C2-C16), while only eleven were detected using FeOx (C1; C2; C5-C8; C12-C16).

Starting with AMX, there are three possible pathways for further degradation. The first one is hydroxylation, which can occur in different positions, yielding the intermediates C5, C7, C11, C15 and C16. From one (C5 and C7) to four hydroxyl groups (C11) are added to the AMX molecule. The assignation of the exact position of these groups is not always possible by the use of the proposed technique, but the observation of the fragmentation pattern can help in this task. Thus, all these intermediates presented the fragment at m/z 160.0431, which corresponds to the thiazolidine ring ($C_6H_{10}NO_2S$; DBE: 2.5) (Fig. 5A). The presence of the same fragment in the mass spectrum of AMX indicates that this moiety remains unchanged and thus the attack of the hydroxyl radicals is expected to occur at the positions in the molecule of AMX more susceptible to an electrophilic attack, i.e. the benzoic ring or the nitrogen atom, with electrons lone pair. The differentiation of the C5 and C7 isomers was possible mainly by the presence of the fragment at m/z 189 in C7 (Fig. 5B). This fragment, which corresponded to the $C_7H_{13}N_2O_2S$ formula (DBE: 2.5) confirmed that the OH attack had no place in the benzoic ring but on the nitrogen atom. This fragment was also present in C15. DBE increase by one unit, observed in C11 and C15 with respect to AMX, was due to oxidation of the amino group to an imino group. This explains the absence of NH_3 loss, characteristic of the AMX and the rest of derivatives containing the amino group.

Another degradation pathway corresponds to the opening of the four-membered β -lactam ring and yields the stereoisomers of penicilloic acid, C1 and C2, and a series of derivatives (C3, C4, C6, C8, C9 and C12), which do not presented the β -lactam ring. C1 and C2 have been already reported as hydrolysis products. A further decarboxylation reaction yielded the intermediates C3 and C4, which were also detected as hydrolysis products. The oxidation of the methyl groups in the thiazolidine ring was evidenced by the identification of the intermediates C8 and C9. C8 showed an increase in the DBE of a unit with respect to C3/C4, while containing an additional oxygen atom. The presence of fragments at m/z 293 ($C_{14}H_{17}N_2O_3S$), m/z 159 ($C_6H_{11}N_2OS$) and m/z 130 (C_5H_8NOS), coming from the decarboxylation and subsequent cleavage of the molecule, confirm this proposal. C9 has been proposed as originated by decarboxylation of C8, however the scarce fragmentation observed in the mass spectrum cannot confirm this structure.

The bond cleavage between nitrogen of the amino group and the carbonyl group is evidenced by compound C10 (m/z 231.0435; $C_8H_{11}N_2O_4S$). The bond cleavage reduced the double-bond equivalency (DBE) from 8.5 to 4.5, due to the loss of benzoic ring and the double bond of the carbonyl group. The next intermediate generated (C13), presents a difference of 2 DBE in relation to C10, due to the loss of the CO group and of the four-membered β -lactam ring. This compound could be also generated by the cleavage of C8 molecule.

Finally, a third degradation route was through the formation of C14 (amoxicillin diketopiperazine 2',5'), an isobaric derivative of AMX generated by the opening of the β -lactam ring with further arrangement of the molecule. Recently, Lamm et al., (2009) have reported by the first time the presence of this derivative in wastewater.

The different iron species influenced the AMX degradation and the intermediates generated. A higher number of intermediates from AMX degradation was observed using $FeSO_4$ when compared to FeOx. Besides, in the presence of FeOx, the intermediates were degraded after 10 min, except the intermediate C13 (45 min), while in the presence of $FeSO_4$ between 15 and 60 min were necessary. However, with both iron species, total degradation of the intermediates determined was observed (Fig. 6). The differences detected between intermediates behavior could be rationalized only from a kinetics (and not mechanistically) point of view. The intermediates not determined in FeOx were those less abundant (C3, C4, C9, C10 and C11) or quickly appearing and degrading since FeOx was a quicker process than $FeSO_4$ (more evident during the first stages of the treatment). The more persistent products were detected during both treatments.

4. Conclusions

Although AMX was more rapidly degraded in the presence of ferrioxalate, the sample presented significant toxicity during all the treatment due to the presence of oxalate. Using $FeSO_4$, significant decrease of toxicity to *Daphnia magna* was observed after 90 min irradiation (from 65% to 5%), when 53% of the TOC was removed. The residual TOC did not contain nitrogen since 100% of the theoretic amount of the total nitrogen was released after 240 min, mainly as ammonium. Sixteen intermediates were identified using HPLC-ESI-TOF, generated after hydroxylation of benzoic ring, opening of β -lactam ring and several other hydroxylation steps. The identification of these intermediates was based on the measurement of the accurate masses of the intermediates and their main fragments. These intermediates were responsible for the toxicity during the treatment, which was then reduced to 45% after 240 min irradiation, when they were converted to short chain carboxylic acids, allowing further conventional treatment.

Acknowledgments

FAPESP, CAPES, CNPq, Spanish Ministry of Education (Contract CONSOLIDER-INGENIO 2010 CSD2006-00044) and Andalusia Regional Government (Project no. P06-TEP-02329).

REFERENCES

- Andreozzi, R., Canterino, M., Marotta, R., Paxeus, N., 2005. Antibiotic removal from wastewaters: the ozonation of amoxicillin. *Journal of Hazardous Materials* 122 (3), 243–250.
- Andreozzi, R., Caprio, V., Ciniglia, C., Champdoré, M., Giudice, R., Marotta, R., Zuccato, E., 2004. Antibiotics in the environment: occurrence in Italian STPs, fate, and preliminary assessment on algal toxicity of amoxicillin. *Environmental Science and Technology* 38 (24), 6832–6838.
- Arslan-Alaton, I., Caglayan, A.E., 2005. Ozonation of procaine penicillin G formulation effluent part I: process optimization and kinetics. *Chemosphere* 59 (1), 31–39.

- Arslan-Alaton, I., Dogruel, S., 2004. Pre-treatment of penicillin formulation effluent by advanced oxidation processes. *Journal of Hazardous Materials* 112 (1–2), 105–113.
- Bautitz, I.R., Nogueira, R.F.P., 2007. Degradation of tetracycline by photo-Fenton process – Solar irradiation and matrix effects. *Journal of Photochemistry and Photobiology A: Chemistry* 187 (1), 33–39.
- Castiglioni, S., Bagnati, R., Fanelli, R., Pomati, F., Calamari, D., Zuccato, E., 2006. Removal of pharmaceuticals in sewage treatment plants in Italy. *Environmental Science and Technology* 40 (1), 357–363.
- Elmolla, E.E., Chaudhuri, M., 2009. Degradation of the antibiotics amoxicillin, ampicillin and cloxacillin in aqueous solution by the photo-Fenton process. *Journal of Hazardous Materials* 172 (2–3), 1476–1481.
- Foti, M., Giacobello, C., Bottari, T., Fisichella, V., Rinaldo, D., Mammina, C., 2009. Antibiotic resistance of Gram negatives isolates from loggerhead sea turtles (*Caretta caretta*) in the central Mediterranean Sea. *Marine Pollution Bulletin* 58 (9), 1363–1366.
- Hatchard, C.G., Parker, C.A., 1956. A new sensitive chemical actinometer II. Potassium ferrioxalate as a standard chemical actinometer. *Proceedings of the Royal Society of London* 235 (1203), 518–536.
- Lamm, A., Gozlan, I., Rotstein, A., Avisar, D., 2009. Detection of amoxicillin-diketopiperazine-2', 5' in wastewater samples. *Journal of Environmental Science and Health. Part A, Toxic/Hazardous Substances & Environmental Engineering* 44 (14), 1512–1517.
- Martins, A.F., Mayer, F., Confortin, E.C., Frank, C.S., 2009. A study of photocatalytic processes involving the degradation of the organic load and amoxicillin in hospital wastewater. *Clean – Soil, Air, Water* 37 (4–5), 365–371.
- Mavronikola, C., Demetriou, M., Hapeshi, E., Partassides, D., Michael, C., Mantzavinos, D., Kassinos, D., 2009. Mineralisation of the antibiotic amoxicillin in pure and surface waters by artificial UVA – and sunlight-induced Fenton oxidation. *Journal of Chemical Technology and Biotechnology* 84 (8), 1211–1217.
- Nagele, E., Moritz, R., 2005. Structure elucidation of degradation products of the antibiotic amoxicillin with ion trap MSⁿ and accurate mass determination by ESI TOF. *Journal of the American Society for Mass Spectrometry* 16 (10), 1670–1676.
- Nogueira, R.F.P., Oliveira, M.C., Paterlini, W.C., 2005a. Simple and fast spectrophotometric determination of H₂O₂ in photo-Fenton reactions using metavanadate. *Talanta* 66 (1), 86–91.
- Nogueira, R.F.P., Silva, M.R.A., Trovó, A.G., 2005b. Influence of the iron source on the solar photo-Fenton degradation of different classes of organic compounds. *Solar Energy* 79 (4), 384–392.
- Pérez-Estrada, L.A., Malato, S., Agüera, A., Fernández-Alba, A. R., 2007. Degradation of dipyrone and its main intermediates by solar AOPs. Identification of intermediate products and toxicity assessment. *Catalysis Today* 129 (1–2), 207–214.
- Pérez-Estrada, L.A., Maldonado, M.I., Gernjak, W., Agüera, A., Fernández-Alba, A.R., Ballesteros, M.M., Malato, S., 2005. Decomposition of diclofenac by solar driven photocatalysis at pilot plant scale. *Catalysis Today* 101 (3–4), 219–226.
- Pintar, A., Besson, M., Gallezot, P., Gibert, J., Martin, D., 2004. Toxicity to *Daphnia magna* and *Vibrio fischeri* of Kraft bleach plant effluents treated by catalytic wet-air oxidation. *Water Research* 38 (2), 289–300.
- Shemer, H., Kunukcu, Y.K., Linden, K.G., 2006. Degradation of the pharmaceutical metronidazole via UV, Fenton and photo-Fenton processes. *Chemosphere* 63 (2), 269–276.
- Trovó, A.G., Melo, S.A., Nogueira, R.F.P., 2008. Photodegradation of the pharmaceuticals amoxicillin, bezafibrate and paracetamol by the photo-Fenton process – application to sewage treatment plant effluent. *Journal of Photochemistry and Photobiology A* 198 (2–3), 215–220.
- Trovó, A.G., Nogueira, R.F.P., Agüera, A., Fernandez-Alba, A.R., Sirtori, C., Sixto, M., 2009. Degradation of sulfamethoxazole in water by solar photo-Fenton. *Chemical and toxicological evaluation. Water Research* 43 (16), 3922–3931.
- Valvo, L., Ciranni, E., Alimenti, R., Alimonti, S., Draisci, R., Giannetti, L., Lucentini, L., 1998. Development of a simple liquid chromatographic method with UV and mass spectrometric detection for the separation of substances related to amoxicillin sodium. *Journal of Chromatography A* 797 (1–2), 311–316.